Author Manuscript

Author Manuscript

Author Manuscript

Author Manuscript

HHS Public Access

Author manuscript

Biomaterials. Author manuscript; available in PMC 2016 November 01.

Published in final edited form as:

Biomaterials. 2015 November ; 70: 23–36. doi:10.1016/j.biomaterials.2015.08.020.

Nutrient-deprived cancer cells preferentially use sialic acid to maintain cell surface glycosylation

Haitham A. Badr[a], **Dina M.M. AlSadek**[b], **Mohit P. Mathew**[c], **Chen-Zhong Li**[d], **Leyla B. Djansugurova**[e], **Kevin J. Yarema**[c,*], and **Hafiz Ahmed**[f,g,*]

[a]Department of Biochemistry, Zagazig University, Zagazig 44511, Egypt

[b]Department of Histology and Cytology, Zagazig University, Zagazig 44511, Egypt

[c]Department of Biomedical Engineering and Translational Tissue Engineering Center, The Johns Hopkins University, 400 North Broadway Street, Baltimore, MD 21231, USA

[d]Department of Biomedical Engineering, Florida International University, 10555 West Flagler Street, Miami, FL 33174 USA

[e]Institute of General Genetics and Cytology, Al-Farabi Ave, 93, Almaty 050060, Kazakhstan

[f]Department of Biochemistry and Molecular Biology, University of Maryland School of Medicine and Institute of Marine and Environmental Technology, 701 East Pratt Street, Baltimore, MD 21202, USA

Abstract

Cancer is characterized by abnormal energy metabolism shaped by nutrient deprivation that malignant cells experience during various stages of tumor development. This study investigated the response of nutrient-deprived cancer cells and their non-malignant counterparts to sialic acid supplementation and found that cells utilize negligible amounts of this sugar for energy. Instead cells use sialic acid to maintain cell surface glycosylation through complementary mechanisms. First, levels of key metabolites (e.g., UDP-GlcNAc and CMP-Neu5Ac) required for glycan biosynthesis are maintained or enhanced upon Neu5Ac supplementation. In concert, sialyltransferase expression increased at both the mRNA and protein levels, which facilitated increased sialylation in biochemical assays that measure sialyltransferase activity as well as at the whole cell level. In the course of these experiments, several important differences emerged that differentiated the cancer cells from their normal counterparts including resistant to sialic acid-mediated energy depletion, consistently more robust sialic acid-mediated glycan display, and distinctive cell surface vs. internal vesicle display of newly-produced sialoglycans. Finally, the impact of sialic acid supplementation on specific markers implicated in cancer progression was demonstrated by measuring levels of expression and sialylation of EGFR1 and MUC1 as well as

[*]Correspondence to: Kevin J. Yarema, 5029 Smith Building, 400 North Broadway Street, Baltimore, MD 21231, USA, Tel: 410-614-6835, Fax: 410-614-6840, kyarema1@jhu.edu. Hafiz Ahmed, GlycoMantra, Inc., 1450 South Rolling Road, Baltimore, MD 21227, USA, Tel: 301-655-1084, Fax: 443-543-5749, hfzahmed86@gmail.com.

[g]Current Address: GlycoMantra Inc., 1450 South Rolling Road, Baltimore, MD 21227, USA

Publisher's Disclaimer: This is a PDF file of an unedited manuscript that has been accepted for publication. As a service to our customers we are providing this early version of the manuscript. The manuscript will undergo copyediting, typesetting, and review of the resulting proof before it is published in its final citable form. Please note that during the production process errors may be discovered which could affect the content, and all legal disclaimers that apply to the journal pertain.

Author Manuscript Author Manuscript Author Manuscript Author Manuscript

the corresponding function of sialic acid-supplemented cells in migration assays. These findings both provide fundamental insight into the biological basis of sialic acid supplementation of nutrient-deprived cancer cells and open the door to the development of diagnostic and prognostic tools.

Keywords

sialic acid; metabolism; lectins; nutrient deprivation; cancer cell; surface sensing

1. Introduction

A long-known feature of cancer is aberrant energy metabolism, exemplified by the Warburg effect wherein cancer cells forego oxidative phosphorylation and instead ferment copious amounts of glucose [1]. Despite renewed interest, including recognition as a next generation “Hallmark of Cancer” in Hanahan and Weinberg’s seminal publication [2], many aspects of abnormal cancer cell metabolism remain unknown. For example, the impact of glucose-driven flux through the hexosamine biosynthetic pathway (HBP) on cell surface glycosylation (Fig. 1) has received little investigation in the context of nutrient deprivation. Nutrient deprivation is common in locally advanced tumors and profoundly influences malignant progression through diverse mechanisms ranging from altering the intracellular glucose metabolism, over-expressions of the sialic acid transporter sialin, and inducing angiogenic factor production [3, 4]. Considering that glucose deprivation reduces flux through the HBP and thus slows the biosynthesis of glycans that drive cancer progression (e.g., highly-branched N-glycans [5] and nucleocytosolic O-GlcNAc [6]), a lack of nutrients could be expected to hinder the development of tumors. However, the existence of cancer as a leading cause of mortality clearly indicates that developing tumors are able to effectively overcome nutrient deprivation. Accordingly, a major impetus of this report is to provide insights into mechanisms that describe how cancer cells maintain the production of glycans that contribute to cancer progression during nutrient deprivation.

A developing tumor actively remodels its microenvironment thereby generating peptides and carbohydrate fragments that can be scavenged by the constituent cancer cells. For example, exogenous amino sugars such as GlcNAc (which are abundant in glycosoaminoglycans found in the ECM) can be salvaged from a cell’s surroundings and incorporated into the HBP (Fig. 1) [7] thereby enabling nutrient-deprived cells to augment nucleotide sugar production. In particular, GlcNAc uptake increases intracellular levels of UDP-GlcNAc, which is a critical building block for not only GlcNAc-containing glycans but also mucin O-glycans and sialic acid (Fig. 1, **1**–**4**). Sialic acid itself can be salvaged from exogenous sources and efficiently taken up by cells [8, 9] and the upregulation of sialin upon nutrient deprivation [3] raises the intriguing possibility that this sugar can be scavenged from a cancer cell’s microenvironment to overcome glucose deficiency. Once taken into cells, sialic acid can be used for cell surface sialylation either directly (Fig. 1A) or via conversion to ManNAc (Fig. 1B). Furthermore, ManNAc can be converted to GlcNAc (Fig. 1C) and the salvage of this sugar into the HBP offers a route by which sialic acid supplementation broadly maintains glycoconjugate biosynthesis by augmenting cellular

Author Manuscript Author Manuscript Author Manuscript Author Manuscript

UDP-GlcNAc levels. Finally, GlcNAc derived from ManNAc in theory can be routed for glycolysis, making it plausible that exogenous sialic acid can be used to replenish cellular energetics (Fig. 1D) during times of nutrient deprivation. This paper establishes that sialic acid supplementation of nutrient-deprived cells primary maintains cell surface glycosylation in general and sialylation in particular. To provide added context for this study, the importance of sialylation is briefly described next.

Sialic acid is a generic name for a family of acidic nine carbon monosaccharides typically found as the outermost units of glycan chains of the glycoproteins [10]. More than fifty chemically distinct sialic acids exist with *N*-acetylneuraminic acid (Neu5Ac) and *N*-glycolylneuraminic acid (Neu5Gc) most common in mammals; humans however cannot synthesize Neu5Gc because of a mutation in the *CMAH* gene that encodes the enzyme that converts CMP-Neu5Ac to CMP-Neu5Gc [11]. Due to their outermost location on cell surface glycans and their widespread occurrence in vertebrate cells, sialic acids are involved ubiquitously in cellular processes ranging from brain development, inflammation, immune response, to tumor metastasis [12]. Aberrant sialylation and altered expression of sialyltransferases are involved in cancer progression and metastasis [13]. Sialic acids are also used as an energy source in bacteria [14] and reports exist that dietary sialic acids play nutritional roles in mammals [15].

The uptake of exogenous sialic acid [8] and its metabolism in mammalian cells (as summarized in Fig. 1) has been extensively documented elsewhere [16]. Here we will focus on the fact that although it has long been known that nutrient deprivation widely exists in tumors because of poor blood supply [3], many aspects of nutrient deprivation in cancer cell metabolism have not been fully elucidated. A particularly sparse area of investigation has been the ability of sialic acid, which in theory can be scavenged from a cell's microenvironment or deliberately introduced using metabolic glycoengineering strategies [16, 17] to ameliorate the impact of nutrient deprivation on intracellular sugar metabolism. In a preliminary communication, we reported the preferential enhancement of sialylation in a breast cancer line compared to normal cells after sialic acid supplementation under conditions of nutrient deprivation [18]. In the current study we expand this line of investigation by using additional malignant and normal cell lines, optimizing the sialic acid supplementation conditions, monitoring the impact of sialic acid supplementation on cellular energetics and nucleotide sugar levels, measuring the expression of genes involved in the sialylation process, and using lectins to visualize whole cell glycosylation patterns. We also show that sialic acid supplementation of nutrient-deprived cancer cells functionally promotes behavior associated with cancer progression (i.e., increased migration on ECM substrates) and that non-human sialic acids show particularly pronounced overexpression in a way that open the door to new diagnostic and treatment options.

2. Materials and Method

2.1. Materials

Sialic acid (*N*-acetyl-5-neuraminic acid, Neu5Ac) was obtained from Santa Cruz Biotechnology (USA). Asialofetuin, collagen type 1, fibronectin, albumin, CMP-Neu5Ac, neuraminidase from *Arthrobacter ureafaciens*, ribonuclease A, insulin, and hydrocortisone

Author Manuscript Author Manuscript Author Manuscript Author Manuscript

were purchased from Sigma-Aldrich (USA). Neu5Gc was purchased from Santa Cruz Biotechnology (USA). RPMI1640 medium (ATCC modification), HEPES buffer, fetal bovine serum (FBS), APO-BrdU TUNEL kit, TRIzol reagent and TO-PRO-3 were purchased from Life Technologies Corporation (USA). Phosphate-buffered saline (PBS, 137 mM sodium chloride, 2.7 mM potassium chloride, 4.3 mM disodium phosphate, 1.4 mM monopotassium phosphate, pH 7.5) was obtained from Technova (USA). Anti-GM130 was from BD Biosciences (USA). *Maackia amurensis* agglutinin I (MAL-I, specific for Neu5Acα2,3Gal) [19], *Sambucus nigra* agglutinin (SNA, specific for Neu5Acα2,6Gal), *Triticum vulgaris* agglutinin (WGA, specific for Neu5Ac and GlcNAc), Succinylated *Triticum vulgaris* agglutinin (SWGA, specific for GlcNAc) and their fluorescein and biotin conjugates and streptavidin-horseradish peroxidase were obtained from Vector Laboratories (USA). Pierce ECL fast western blots kit and cover slips were purchased from Thermo Fisher Scientific (USA). The ATP assay kit was obtained from Molecular Probes (USA). All other chemicals were purchased from Sigma-Aldrich in analytical grade quality.

2.2. Cell lines and culture conditions

Human normal mammary epithelial cell lines MCF10A and HB4A and breast cancer cell lines T47D, MCF7 and MDA MB231 (American Type Culture Collection, USA) were cultured in 175 cm^2 flasks in RPMI1640 medium (without added antibiotics to avoid sialyltransferase inhibition [20]), supplemented with 1% FBS (to minimize the interference degree of BSA sialylation) at 37 °C under 5% CO_2. For normal cells, the medium also contained 10 μg/mL insulin and 5 μg/mL hydrocortisone. For all experiments, MCF10A, HB4A, T47D, MCF7 and MDA MB231 cells were used within the first three passages, incubated 72 h to reach mid-exponential growth phase, and harvested by treatment with 5 ml of buffer containing 0.54 mM EDTA, 154 mM NaCl, and 10 mM *N*-2-hydroxyethylpiperazine-*N*-2-ethane sulfonic acid (HEPES), pH 7.4 for <5 min at 37 °C.

2.3. Nutrient deprivation and Neu5Ac treatment

Protocol for nutrient deprivation of cells in suspension—Step 1, cell cultures were harvested as described in Section 2.2 above. Step 2, cells were resuspended in serum-free RPMI-1640 medium and pelleted by centrifugation at 900 ×g for 5 min; during this step cells experience 10 min of nutrient deprivation in serum-free media without Neu5Ac. Step 3, the cells were rinsed twice in 37 °C PBS by centrifugation for 5 min and 1 mL aliquots of 1 × 10^4 cells were pipetted gently into 15 mL BD Falcon tubes; during this step the cells experience an additional 20 min of nutrient-deprivation. Step 3, cell suspension aliquots corresponding to 10^4 cells mL^{-1} were equilibrated in tubes containing Neu5Ac-PBS buffer by placing the tubes with opened caps for 60 min in a humidified incubator at 37°C and 5% CO_2 with continuous shaking at 30 strokes per minute; during this Neu5Ac-supplementation step, negative controls were maintained in non-supplemented PBS. Step 4, the Neu5Ac-PBS solution was decanted, the tubes were gently tapped to loosen the gravity-pelleted cells, and then rinsed twice in warm (37 °C) PBS followed by pelleting by 5 min of centrifugation each time; this process provided an additional 30 min of nutrient-deprivation in the absence of supplemental Neu5Ac. The entire 5 step process results in 2 h of nutrient deprivation, after which the cells were analyzed by the methods listed below with the exception of the

Author Manuscript Author Manuscript Author Manuscript Author Manuscript

wound healing assays (Section 2.10) and lectin staining (Section 2.11) which used cells that were nutrient-deprived under adherent conditions.

Protocol for nutrient deprivation of adherent cells—Step 1, cells were cultured on sterile glass microscope cover slips for two days. Step 2, the cover slips were placed in a sterile plastic rack in warm (37 °C) PBS buffer for 30 min, then the PBS was replaced with Neu5Ac-PBS solution for 60 min to provide Neu5Ac supplementation (controls were maintained in non-supplemented PBS), and then the cell-laden cover slips were placed back in PBS buffer for 30 min. All incubations were performed in a humidified incubator at 37°C and 5% CO_2 with continuous shaking at 30 strokes per minute. Overall this process mimics the non-adherent treatment conditions with respect to the duration of nutrient-deprivation (2 h total) and Neu5Ac supplementation (60 min).

In addition to the nutrient-deprivation protocols, “nutrient-happy” control experiments were performed where the cells were maintained in serum containing medium and treated with Neu5Ac (or not for the Neu5Ac(−) controls) as described above.

2.4. Neu5Gc treatment

Cells were split and cultured (before feeding experiments) in RPMI1640 medium supplemented with 1% heat-inactivated human serum (RPMI/HUS) instead of FBS, resulting in chase-out of existing Neu5Gc [21]. Subsequently, cells were fed with 10 mM Neu5Gc in RPMI/HUS medium or under nutrient deprived conditions as described above.

2.5. Cell viability assay

Cells were harvested as described above without fixation. Cell pellets were resuspended in PBS supplemented with 1 mg/mL propidium iodide (PI) and incubated for 5 min at ambient temperature. Cells were analyzed by flow cytometry on BD Accuri C6 flow cytometer with CFlow Plus operating software (BD Biosciences, USA). The proportion of dead and living cells was determined as the percentage of PI-stained cells. The MTT assay was used to measure changes in cell viability and proliferation for 5 days after returning the Neu5Ac-treated and untreated cells to the complete medium. The formazan dye produced after DMSO solubilization was quantified at 560 nm using a multiwell scanning spectrophotometer (Bio-Rad, USA).

2.6. Quantification of CMP-Neu5Ac, UDP-GlcNAc, surface Neu5Ac, and surface Neu5Gc

PBS-washed cells (1×10^6) (untreated or Neu5Ac treated) were lysed by hypotonic shock in 1 mL water (15 min, 4°C). The intracellular cytidine-5′-monophospho-*N*-acetylneuraminic acid (CMP-Neu5Ac) and uridine-5′-diphospho-*N*-acetyl-D-glucosamine (UDP-GlcNAc) were purified from the cell lysates and analyzed by ion-pair reversed-phase high performance liquid chromatography (IP RP HPLC) using a ODS column as described [22]. Cell membrane-bound Neu5Ac (from untreated and Neu5Ac treated) and Neu5Gc (from untreated and Neu5Gc treated) were determined by acid hydrolysis followed by derivatization with 1,2-diamino-4,5-methylenedioxybenze (DMB) and HPLC separation as previously described [9, 23]. The content of CMP-Neu5Ac, UDP-GlcNAc, surface Neu5Ac,

Author Manuscript Author Manuscript Author Manuscript Author Manuscript

and surface Neu5Gc was shown in nano mole per mg cell protein from five independent experiments.

2.7. Detection of sialyltransferase activity

The activity of α2→3-sialyltransferase (α2→3-ST) and α2→6-sialyltransferase (α2→6-ST) to galactose was determined with a solid phase assay using asialofetuin-precoated plates as previously described [24]. Briefly, various cell lysates containing equal amount of protein were placed into the wells and CMP-Neu5Ac was then added to initiate the reaction. After washing and blocking, the sialylated fetuin was allowed to interact with either biotinylated lectin (MAL-I or SNA) followed by binding with streptavidin-horseradish peroxidase. The negative control included only lectin binding to asialofetuin. After binding and washing, the reaction was developed with 100 μL of substrate (0.03% H_2O_2, 2 mg/mL *o*-phenylenediamine in 0.1 mM citrate buffer, pH 5.5) for ~10 min and terminated with 1 M H_2SO_4. The absorbance at 492 nm was measured using an automatic multiwell spectrophotometer (Bio-Rad, USA).

2.8. Gene expression analyses by reverse transcriptase polymerase chain reaction (RT-PCR) and quantitative RT-PCR

Total RNA was extracted from cells using TRIzol reagent and 1 μg of total RNA was reverse transcribed to cDNA using the GoScript™ Reverse Transcription System (Promega, USA). The resulting cDNA was amplified in triplicate using GoTaq qPCR Master Mix (Promega, USA) on a Real-Time PCR System (Applied Biosystems, USA). β-Actin was used as the internal control. The relative expression levels were analyzed in Microsoft Excel using the comparative $2^{-\Delta\Delta CT}$ method as per the instructions of the manufacturer (Applied Biosystems). The primer sequences for ST3Gal-III, ST3Gal-IV, ST6Gal-I, CMP-Neu5Ac synthetase, Mucin1 (MUC1), epidermal growth factor receptor (EGFR), and β-Actin were previously reported [25–28].

2.9. Flow cytometry analysis

For this purpose, cells were fixed by suspending them in 70% (*v/v*) ethanol and stored at 4°C for 15 min, washed twice with cold PBS, and then placed in 96-well plates (1×10^4 cells per well). The cells were then stained with the fluorescein isothiocyanate-labeled lectins (SWGA, WGA, SNA and MAL-I). For the comparison of mean fluorescence intensities, the instrument settings for fluorescence and compensation were the same for all experiments. Data were collected from at least 10,000 cells for each sample. For TUNEL assay, cells were incubated with DNA-labeling solution (10 μL reaction buffer, 0.75 μL TdT enzyme, 8 μL BrdUTP, 31.25 μL of dH_2O) for 1 h at 25°C. Each sample was then exposed to an antibody solution consisting of 5 μL Alexa Fluor 488 labeled anti-BrdU antibody with 95 μL rinse solution and allowed to react for 20 min.

2.10. Wound healing assays

For this purpose, two sets of each cell monolayer were scratched using a pipette tip [29]. One set of each cell was treated with 10 mM Neu5Ac in PBS for 2 h as described above in “Neu5Ac treatment” and after washing, the cells were incubated in the complete medium for

Author Manuscript Author Manuscript Author Manuscript Author Manuscript

additional 24 h at 37°C. Cell migration, which was considered as wound healing, was quantitated as based on the number of cells that entered an area of the wound following a previously-described protocol [30].

2.11. Lectin staining and cell imaging

Cells were grown on the surface of a cover slip and the adherent cells were fixed with 70% ice-cold ethanol for 15 min. After washing with PBS, cells were stained with different FITC-labeled lectins (5 μg/mL) for 1 h. To visualize Golgi markers, the cells were then incubated with anti-GM130 conjugated to Alexa Fluor 647. After staining, cells were further treated with Ribonuclease A (10 μg/mL) and the nuclei were counter stained with TO-PRO-3. Images were captured on DV elite imaging system and merged using softWoRx DMS from Applied Precision (Applied Precision, USA).

2.12. Western blotting, immuno-precipitation and lectin-precipitation

Cells were lysed in Triton X-100 lysis buffer (10 mM Tris-HCl [pH 8.0], 5 mM ethylenediaminetetraacetic acid, 320 mM sucrose, 1% Triton X-100, 1 mM PMSF, 2 mM DTT, 1 μg/mL leupeptin, 1 μg/mL aprotinin) and then incubated on ice for 15 min. Following centrifugation, the supernatant was collected and protein concentrations were determined by BCA protein assay kit (Pierce). For each sample, 50 μg total lysate was separated by SDS-PAGE and transferred onto PVDF membranes (Pierce) following standard procedures. After incubation with primary antibodies [specific for CMP-Neu5Ac synthetase (sc-167497 Santa Cruz), ST3Gal-III (H-6487-B01P Novus), ST3Gal-IV (H-6484-M01 Novus), ST6Gal-I (H-6480-M01 Novus), Mucin1 (sc-7313 Santa Cruz), epidermal growth factor receptor (EGFR 2232 Cell Signaling), and β-Actin (sc-47778 Santa Cruz)], the blots were incubated with corresponding secondary antibody-horseradish peroxidase (HRP) conjugate (Santa Cruz) and signals were detected by ECL system (Pierce). Negative control includes PBS instead of primary antibody. For immuno-precipitation, each cell extract (100 μg of total protein) was incubated with 1 μg of either anti-MUC1 antibody or anti-EGFR antibody. The precipitated protein was subjected to SDS-PAGE and Western blotting followed by the detection with the corresponding antibody as described above. For precipitation of α2→3/6-sialylated glycoproteins with SNA and MAL-I, each cell extract (100 μg of total protein) was incubated with 1 μg lectin. The precipitated protein was separated on SDS-PAGE followed by Western blot detection with anti-MUC1 and anti-EGFR antibodies as described above. Precipitation experiments were also performed with the desialylated protein extract and similar blots were prepared. For desialylation, the cell extract was incubated with neuraminidase (100 mU/mL) for 1 h at 37 °C.

2.13. ATP assay

MCF-10A or MDA MB231 cells (3×10^6 cells) were suspended in 10 mL of serum free media or PBS supplemented with 10 mM Neu5Ac or 10 mM glucose. After 2 h incubation, the cells were harvested and washed in PBS. ATP was extracted using boiling deionized water [31] and measured on a luminescence plate reader using the ATP determination Kit (Molecular Probes) following the protocols supplied by the manufacturer.

Author Manuscript Author Manuscript Author Manuscript Author Manuscript

2.14. Statistical analysis

Data are expressed as the mean S.E. for at least five independent experiments. Statistical significance of differences between means was determined by analysis of variance. The differences were considered significant when $p<0.05$.

3. Results

3.1. Effect of nutrient deprivation on cell viability

Conditions were optimized to determine the maximum duration that cells could withstand nutrient deprivation without cytotoxicity in MCF10A (normal mammary epithelial cells) and cancerous MCF7 or MDA MB231 cells. First a TUNEL assay compared the normal MCF10A and cancerous MCF7 cells over a 240 min time course of nutrient deprivation; negligible cytotoxicity occurred up to 120 min but cell death became measurable at 180 and 240 min (Fig. 2A with representative flow cytometry traces given in Fig. S1A). These results were corroborated by confocal microscopy (Fig. 2B). Next, to ensure these results extended across additional cell lines as well as to sialic acid supplemented cells, all five cell lines used in this report were analyzed by the TUNEL assay with and without Neu5Ac treatment during 120 min of nutrient deprivation; the proportion of viable cells was 93–96% in all cases (Fig. 2C with quantification in Fig. S1B). Once it was established that cell viability was maintained for 120 min of nutrient deprivation with or without supplementation with 10 mM Neu5Ac, a two hour time period was used in all further experiments; of note (and relevant to experiments reported later in Fig. 5), 2 h was sufficient to restore surface sialylation in nutrient-deprived cells (Fig. S1C). The concentration of Neu5Ac used in this and all successive experiments was 10 mM, a concentration that dose dependence experiments established to provide a maximal response (Fig. S1D).

3.2. Sialic acid supplementation does not restore ATP production in nutrient-deprived cells

Next, the energetics of a normal (the MCF10A) and a cancerous (MDA MB231) line were evaluated by comparing cells supplemented with glucose or Neu5Ac in normal medium or PBS (i.e., nutrient deprivation conditions). The addition of 10 mM of glucose to MCF10A cells maintained in complete medium that already had ~25 mM glucose resulted in slightly reduced ATP levels after 2 h (Fig. 3A); an explanation is that the excessive levels of glucose essentially mimic “diabetic” conditions causing these cells to compensate by restricting glucose uptake. In PBS however, the slight deficit of ATP in the nutrient-deprived cells was compensated by addition of 10 mM glucose, restoring levels to cells maintained continuously in normal media. Unlike for glucose, the addition of 10 mM Neu5Ac to the MCF10A cells maintained in normal media had no effect on ATP levels (Fig. 3B), suggesting that this sugar did not have a synergistic effect or overlapping function with glucose (i.e., it was not used for energy production). The addition of Neu5Ac to nutrient-deprived MCF10A cells completely depleted ATP levels confirming that this sugar was not used for energy production.

Supplementation of the MDA MB231 cells with glucose and Neu5Ac illustrates another facet by which cancer cells have dramatically different monosaccharide metabolism compared to normal cells. In particular, addition of 10 mM glucose to normal media did not

Author Manuscript Author Manuscript Author Manuscript Author Manuscript

have a measurable effect on ATP levels (Fig. 3C) unlike in the normal cells where levels were slightly depleted. This result is consistent with the Warburg effect where cancer cells metabolize large amounts of glucose. Consistent with the robust requirements for glucose of cancer cells, the nutrient-deprived MDA MB231 cells experienced a greater level of ATP depletion after 2 h in PBS compared to the MCF10A cells; ATP levels were restored to normal levels by 10 mM glucose supplementation. Neu5Ac supplementation, however, failed to change ATP levels in MDA MB231 cells maintained either in complete media or in PBS (Fig. 3D) unlike in the nutrient-deprived normal cells where Neu5Ac supplementation completely depleted ATP (Fig. 3B). Of note, nutrient depletion with or without sialic acid supplementation did not have long term (5 day) consequences on cell viability after the cells were returned to normal media (Fig. S2).

3.3. Sialic acid supplementation increases nucleotide sugar levels and augments sialylation

The most straightforward fate of exogenously-supplemented Neu5Ac is conversion to CMP-Neu5Ac (Fig. 1A), which is then used as the co-substrate for sialyltransferases that attach this sugar to cellular glycoconjugates; an alternative metabolic route allows sialic acid to be converted to ManNAc (Fig. 1B) and then routed into an earlier stage of the sialic acid pathway [9]. Either way, intracellular pools of CMP-sialic acids would be expected to increase upon Neu5Ac supplementation, which we experimentally demonstrated by analysis of nutrient deprived cells where levels of this nucleotide sugar increased for all cell types tested (0.45, 0.51, 1.06, 2.253, and 2.496 nano mole/mg protein for MCF10A, HB4A, T47D, MCF7 and MDA MB231, respectively) compared to the corresponding untreated cells (0.29, 0.33, 0.422, 0.75 and 0.78 nano mole/mg protein) respectively (Table 1A). The enhancement of CMP-Neu5Ac in the Neu5Ac treated malignant cells (T47D, MCF7 and MDA MB231; 2.5–3.2 fold respectively) was stronger than in the normal cells (MCF10A and HB4A, ~1.5 fold) (Table 1A).

We next tested whether the higher amounts of CMP-Neu5Ac in Neu5Ac-supplemented, nutrient-deprived cells increased levels of glycoconjugate-bound sialic acid. The content of the membrane-bound sialic acid was 2–2.5-fold higher in nutrient-deprived malignant cells when treated with Neu5Ac (10 mM, 2 h) (Table 1B) whereas Neu5Ac supplementation of nutrient-deprived normal cells only led to an increase of ~1.3 to 1.4-fold (Table 1B). It is noteworthy that the starting levels of sialic acid were lower in the normal cells, resulting in the final levels in the cancer cells being as much as 4-fold higher.

We next investigated whether exogenously-supplied Neu5Ac, after conversion to ManNAc by NPL (Fig. 1B) and then to GlcNAc (Fig. 1C), can be salvaged by the HBP thereby maintaining or even increasing intracellular levels of UDP-GlcNAc. By using HPLC measurements, we found an increase in UDP-GlcNAc of 2-fold or more in all cell types, with the already-higher levels in the cancer lines (T47D, MCF7, and MDA MB231) increasing by almost 3-fold in some cases (Table 1 C). In addition to these measurements taken immediately after 2 h of nutrient deprivation, the levels of nucleotide sugars and glycan-displayed sialic acids were monitored for 8 and 24 h after cells were returned to normal complete media (Table S1). After 24 h most parameters had equalized between the

Author Manuscript Author Manuscript Author Manuscript Author Manuscript

treated and non-supplemented cells for both MCF10 normal cells (Table S1 A) and MCF7 cancer cells (Table S1 B), except for CMP-Neu5Ac levels, which stayed persistently higher in the supplemented cells. A plausible explanation is that cells have no other metabolic option for CMP-Neu5Ac, a generally tightly controlled metabolite, other than for use as a co-substrate for sialyltransferases and therefore excess amounts cannot be quickly ameliorated.

3.4. Neu5Gc supplementation leads to robust glycoconjugate incorporation

To investigate whether normal and malignant cells incorporate Neu5Gc (a form of sialic acid not naturally produced by human cells) in a similar manner to Neu5Ac, both cell types were treated with 10 mM Neu5Gc for 2 h under nutrient-deprived conditions. Untreated cells showed low but measurable residual levels Neu5Gc (0.13–0.29 nmole/mg protein), which is likely a consequence of these cells previously been cultures with bovine serum that is a rich source of Neu5Gc. The treated cells nevertheless showed significant uptake of Neu5Gc (0.17–1.21 nmole/mg protein) (Table 1D) with the uptake in normal cells (MCF10A and HB4A) only slightly increasing (e.g., by 1.3 or 1.4-fold) over Neu5Gc levels while malignant cells (T47D, MCF7, and MDA MB231) showed 3–6 fold higher levels.

3.5. Neu5Ac treatment increases expression of CMP-Neu5Ac synthetase and sialyltransferases

The increase in sialoglycans in Neu5Ac treated cells was consistent with enhanced levels of CMP-Neu5Ac but it remains controversial how much of a role this nucleotide sugar plays in cell surface glycosylation because it is often assumed that sialylation is primarily controlled by sialyltransferase expression and activity. Therefore, we investigated whether transcriptional control of these relevant enzymes played a role in the increased sialylation observed in nutrient-deprived cells by measuring mRNA expression levels of CMP-Neu5Ac synthetase and sialyltransferases by quantitative RT-PCR. The mRNA levels of CMP-Neu5Ac synthetase in Neu5Ac-treated cell lines increased approximately 2-fold when compared to the corresponding untreated cells (Fig. 4A), which is consistent with the increased levels of CMP-Neu5Ac observed and also indicates that cells have a “feed-forward” regulatory mechanism for utilizing sialic acids for glycosylation when this sugar is abundant.

Similarly, the mRNA levels of ST3Gal-III, ST3Gal-IV, and ST6Gal-I also increased in all nutrient-deprived lines that had been supplemented with Neu5Ac by at least 1.5-fold when compared to the corresponding untreated cells. In several cases, however, particularly in the malignant cells, much higher levels of sialyltransferase mRNA expression were observed (e.g., 3.7 to 9.6-fold compared to the corresponding untreated cells, Fig. 4A). The changes in mRNA levels were validated by Western blots where increased expression of CMP-Neu5Ac synthetase, ST3Gal-III, ST3Gal-IV, and ST6Gal-I proteins was observed (Fig. 4B). The primary antibodies used in these blots were very specific to the corresponding protein and only one band base detected in each case; moreover, the negative control for each blot showed no bands (data not shown). Finally, to confirm Neu5Ac supplementation actually influences sialyltransferase activity during nutrient deprivation, cell extracts were incubated with asialofetuin (which acts as sialic acid acceptor) and the resultant sialofetuin was

Author Manuscript Author Manuscript Author Manuscript Author Manuscript

analyzed using linkage-specific lectins and both α2→3-ST and α2→6-ST activities increased by 29–79% (Fig. 4C). Together with enhanced CMP-Neu5Ac (Table 1), these expression and activity data demonstrate Neu5Ac supplementation triggers a multifaceted response capable of maintaining glycosylation, especially sialylation, in nutrient-deprived cells with this effect being noticeably more pronounced in cancer compared to normal cell lines. We next performed lectin binding and behavioral assays of Neu5Ac-treated nutrient-deprived cells to confirm that the biochemical and enzyme-based analysis have significance at the cell level.

3.6. Lectin binding confirms that Neu5Ac supplementation modulates cell surface glycosylation

To verify that the increased abundance of nucleotide sugars and expression of sialyltransferases in Neu5Ac-treated, nutrient-deprived cells modulates cell surface glycosylation, we performed lectin binding assays. First, we tested binding of succinylated WGA (sWGA, Fig. 5A) and found increased affinity of this GlcNAc-binding lectin to all Neu5Ac-supplemented cells, consistent with the increased UDP-GlcNAc levels reported in Table 1. Beyond confirming this one endpoint consistent with increased UDP-GlcNAc (i.e., sWGA staining), fully exploring the impact of this nucleotide sugar on overall cell glycosylation is incredibly complex (as outlined in Fig. 1, routes **1**, **2**, **3**, and **4**) and was beyond the scope of the current study. Instead, we focused further efforts on sialylation and similarly found increases in cell surface binding for WGA (Fig. 5B), a lectin that binds to both α2,3- and α2,6-linked sialic acid with slightly greater enhancement in the malignant cells (T47D, MCF7 and MDA MB231) compared to the normal lines (MCF10A and HB4A). Upon using lectins that discriminate between α2,3- and α2,6-linkages, SNA binding to α2,6-sialic acids (Fig. 5C) revealed roughly proportional increases in all lines whereas MAL-I binding to α2,3-linked sialic acid (Fig. 5D) showed greater enhancement in the malignant lines compared to the normal cells. In control experiments, both normal and malignant cells treated with Neu5Ac (10 mM for 48 h) in complete medium showed only minimal enhancement (e.g., 6–28%) of lectin binding that was due primarily to an increase in α2,6-linked sialosides (Fig. S3). This result was not surprising because when cellular levels of UDP-GlcNAc are adequate, flux of ManNAc into the sialic acid pathway is not limiting; therefore cells maintained under normal conditions are thought to have saturating levels metabolic intermediates required for sialylation [17].

The increased lectin binding to the Neu5Ac-supplemented, nutrient-deprived cells was corroborated by confocal microscopy. Consistent with the flow cytometry data, FITC-conjugated WGA and SNA lectins showed a strong fluorescence signal for both normal and cancer cells, and the fluorescence intensity was further enhanced after sialic acid treatment (Fig. 5E). MAL-I bound weakly to the normal cells (untreated or treated) and also to untreated malignant cells, however, stronger staining (e.g., up to 2.8-fold) was observed in sialic acid treated malignant cells. Interestingly, MAL-I staining in the treated normal cells was distributed throughout the Golgi as demonstrated by co-localization with the Golgi marker GM130, but in the malignant cells this lectin was located almost exclusively on the cell surface (Fig. 5F).

Author Manuscript Author Manuscript Author Manuscript Author Manuscript

3.7. Neu5Ac treatment increases the expression and sialylation of EGFR and MUC1

To explore the importance of sialic acid supplementation of nutrient-deprived cells on specific membrane glycoproteins, two cell surface receptors (EGFR and MUC1) were chosen because of their important roles in promoting tumor growth and metastasis, which have previously been investigated in our laboratories [32, 33]. To verify that EGFR and MUC1 were over-expressed, over-sialylated, or both EGFR and MUC1 were immuno-precipitated and analyzed by Western blot analysis using commercial antibodies that recognized the un-glycosylated form of each protein. The murine-raised anti-MUC1 recognizes an epitope corresponding to the tandem repeat region of MUC1and detects only one band in MCF7 cell line (Product Data Sheet, Santa Cruz) as well as in other cell lines (Personal Communication, Santa Cruz Technical Service). Anti-EGFR antibody also detected only one band. Negative control experiment for each antibody did not result any band (data not shown). As shown in Figure 6A, anti-MUC1 and anti-EGFR antibodies immuno-precipitated increased amounts of MUC1 and EGFR from malignant cell lysates compared to the normal cells.

The higher levels of MUC1 and EGFR immunopurified by antibodies that recognize protein epitopes of these glycoproteins was consistent with qRT-PCR results where mRNA levels of these two proteins in nutrient-deprived cells supplemented with sialic acid were compared to the untreated cells (Fig. S4). Moreover, MUC1 and EGFR purified from the Neu5Ac treated malignant cells were more heavily sialylated (based on slower migration observed during SDS-PAGE) compared to those from the untreated cells, an effect that was reversed by sialidase treatment (Fig. 6A). To further corroborate the increased sialylation of these cancer markers, equal amounts of immunoprecipitated MUC1 and EGFR were precipitated with MAL-I and subjected to Western blot analysis followed by immunodetection that again showed that the malignant cells migrated slower during SDS-PAGE consistent with increased sialylation (Fig. 6B). The increased sialylation of MUC1 and EGFR was a least in part due to $\alpha 2\rightarrow 3$ sialic acids because these immunoprecipitated glycoproteins were further precipitated by MAL-I. To confirm MAL-I specificity towards Neu5Ac$\alpha 2\rightarrow 3$Gal, equal amounts of desialylated immunoprecipitated glycoproteins (asialoMUC1 and asialoEGFR) were precipitated with MAL-I and subjected to Western blot followed by immunodetection (Fig. 6B).

3.8. Neu5Ac treatment modulates cellular functions associated with EGFR and MUC1

As a final part of this study, we reasoned that that the elegant mechanisms we uncovered and described above by which cancer cells maintain cell surface sialylation and the expression of genes implicated in cancer progression even during nutrient deprivation must be in place to confer functional advantages during tumor development and carcinogenesis. Based on established connections between cell surface sialylation and the metastatic potential of breast cancer cells, we conducted wound healing assays that measure cell motility to verify that the increased sialylation that occurs in nutrient-deprived, sialic acid-supplemented cells affects cell adhesion in ways that can promote cancer progression. As shown in Figure 6C, the migration of Neu5Ac-treated malignant cells markedly increased when cells were placed on substrates coated with collagen type I and fibronectin, but not with the BSA controls.

Author Manuscript Author Manuscript Author Manuscript Author Manuscript

4. Discussion

Unique metabolic properties of tumor cells – in particular their propensity to forgo oxidative phosphorylation and instead use copious amounts of glucose for energy metabolism – are now recognized as a hallmark of cancer [2]. As outlined in Figure 1 the consequences of the Warburg effect include increased flux through the HBP, which can profoundly affect cell surface glycosylation patterns that we (and others) have been attempting to exploit as biomarkers of cancer through various methods including lectin binding [34, 35] and surface plasmon resonance [35, 36]. Moreover, differences in cancer cell glycosylation can be exacerbated by nutrient deprivation (which in effect reverses Warburg effect-driven flux through the HBP) combined with supplementation with exogenously-supplied sialic acid [18].

As discussed in more detail below, the current report builds on these previous findings in several important ways. First, energy metabolism and metabolic intermediates were evaluated in nutrient-deprived cancer cells in experiments that showed that sialic acid supplementation did not restore energy supplies in cells but instead augmented levels of nucleotide sugars required for glycosylation. Second, qRT-PCR and Western analysis of sialyltransferases showed that sialic acid supplementation rapidly enhanced the expression of these enzymes in a way that complemented CMP-Neu5Ac levels and increased surface sialylation. Third, the expression and sialylation of MUC1 and EGFR were increased upon sialic acid supplementation showing functional relevance of these endpoints. Fourth, supplementation with the non-human Neu5Gc form of sialic acid resulted in especially pronounced surface incorporation suggesting that “metabolic glycoengineering” strategies [16] carried out under conditions of nutrient deprivation may be particularly promising for biomarker detection or sialic acid-based treatment strategies [32]. Finally, several cell lines were evaluated showing that differences between cancer and normal cells were broad-based. The time frame of the experiment (2 h) is consistent with the kinetics of incorporation of exogenously supplied sialic acids and surface display as previously reported [37].

The restoration of surface glycosylation after sialic acid supplementation of nutrient-deprived cells in theory could result from the routing of this sugar into energy production based on metabolic pathway connections shown in Figure 1. This possibility, however, was ruled out by observing that no increase in ATP levels occurred upon sialic acid supplementation whereas glucose effectively restored ATP in nutrient-deprived cells. Quite strikingly, in contrast to putatively increasing ATP levels, sialic acid supplementation completely depleted the already low levels of ATP in the normal MCF10A line. This result can be explained by the increased levels of nucleotide sugars (CMP-Neu5Ac and UDP-GlcNAc) in the treated cells that require the input of high energy co-substrates during their biosynthesis. The lack of further ATP depletion in the Neu5Ac-treated MDA MB231 cells suggests that the cancer cells have effective coping mechanisms for maintaining surface sialylation under nutrient deprivation, which is consistent with the many important roles that this sugar plays in cancer progression.

The underlying mechanism behind the dramatic differences in ATP levels in the cancer and normal lines upon sialic acid supplementation remains unclear but the experiments shown in

Author Manuscript Author Manuscript Author Manuscript Author Manuscript

Figure 2 strongly discount the possibility that exogenously-supplied sialic acid was used for energy in either type of cell. Therefore, we focused on other possible metabolic fates for exogenously-supplied Neu5Ac. The simplest fate is direct conversion to CMP-Neu5Ac consistent with the elevated levels of this nucleotide sugar observed in sialic acid treated cells (Table 1). Alternatively, exogenously-supplied sialic acid can be catabolized to ManNAc and pyruvate [9] and then converted back to sialic acid and used for surface sialylation. Another fate for ManNAc is conversion to GlcNAc [32] that in turn can be salvaged by the HBP; this metabolic route is consistent with the increased levels of UDP-GlcNAc observed in the treated cells (Table 1).

The ability of exogenously-supplied sialic acid to augment dwindling levels of UDP-GlcNAc in nutrient-deprived cells is significant on multiple levels. First, because this nucleotide sugar is a feedstock required for the production of virtually all glycoconjugates (Figure 1, steps **1**, **2**, **3**, & **4**), the overall display of cell surface glycans is maintained or even enhanced by the increased level of this nucleotide sugar that occurs upon sialic acid supplementation. This feature is important because sialylation is a terminal modification that requires underlying glycan structures. Therefore if sialic acid supplementation only directed metabolic flux to CMP-Neu5Ac production, surface sialylation could not be rescued in nutrient-deprived cells if the underlying glycans that depend on UDP-GlcNAc for biosynthesis – and that serve as acceptor sites for sialic acid – were deficient. Therefore, the bidirectional flux of exogenous sialic acid towards both UDP-GlcNAc and CMP-Neu5Ac biosynthesis comprises a multifaceted strategy that allows cells to maintain surface sialyation.

Another important role for UDP-GlcNAc in cells is to serve as a “nutrient sensor” that is transduced to many aspects of cellular physiology in a very dynamic fashion through O-GlcNAc modified proteins [36] but prior to the information presented in this report, it has not been known that sialic acid comprises one of the nutrients critical to regulating this central controlling molecule. We found evidence that O-GlcNAc can epigenetically control transcription [39] particularly intriguing because sialic acid-driven changes to UDP-GlcNAc levels therefore plausibly have the ability to modulate gene expression and explain the transcriptional responses we observed throughout this study. We were interested in gene expression because of ambiguity over whether increased levels of CMP-Neu5Ac can affect cell surface sialylation; in particular because the Golgi concentration of CMP-Neu5Ac exceeds the K_m for sialyltransferases it has been thought that enhanced CMP-Neu5Ac levels do not translate into increased sialylation of glycoconjugates [16]. Increasing evidence however, including results from our team [30], indicates that metabolic flux by itself can influence cell surface sialylation patterns. Regardless of these ambiguities, clearly the synergistic up-regulation of sialyltransferase expression along with increased CMP-Neu5Ac – both of which we observed in the sialic acid treated nutrient-deprived cells – provides an ideal scenario for the biosynthesis of sialoglycoconjugates. Indeed, we found increased sialyltransferase activity by measuring sialoglycoconjugate formation in biochemical assays (Fig. 4C) as well as increased sialylation at the whole cell level by lectin staining that revealed increases in overall sialylation (WGA staining, Fig. 5B) as well as α2,6 and α2,3-linked sialic acids (SNA and MAL-I, respectively, Fig. 5C, D) consistent with the

Author Manuscript Author Manuscript Author Manuscript Author Manuscript

upregulation of both α2,3-sialyltransferases such as ST3Gal I, ST3Gal III, ST3Gal IV, ST3Gal VI, and α2,6-sialyltransferases such as ST6Gal in many cancers including breast, pancreatic, ovarian, and cervical cancers [13, 40–42].

Although differential cell surface sialylation during cancer transformation and progression already is well known [43], this study provides important new information describing how malignant cells respond when they are deprived of nutrients. As described above at a biochemical level, sialic acid supplementation of nutrient-deprived cells dramatically rescued cell surface sialic acid display, which assists tumor development in many ways. Importantly, the enhanced expression of ST3Gal-I and ST6GalNAc-I – which was observed in this study – increases the tumorigenicity of breast cancer cells [44]; for example, one relevant endpoint is that sialylation promotes cell detachment from primary tumors through charge repulsion thereby promoting proliferation and migration. Here, we showed that the mobility of sialic acid-treated malignant cells markedly increased on collagen type I and fibronectin substrates (Fig. 6) thereby confirming that supplementation with this sugar functionally contributes to an endpoint relevant to cancer progression.

The majority of this study was devoted to gaining insight into fundamental biology of sialic acid supplementation of nutrient-deprived cells and many similarities were found between cancer and normal breast lines. However, a handful of distinctive qualitative differences did emerge, including the rapid and complete depletion of ATP in sialic acid treated normal cells (while cancer cells were refractory to this effect, Fig. 3) and the surface display of rescued sialoglycoconjugates in cancer cells compared to their retention in internal bodies in the normal lines (Fig. 5F). More generally, the critical difference between cancer and normal lines was quantitative in nature, with consistently stronger responses to sialic acid supplementation observed in cancer cells. Particularly pronounced was the response of nutrient-deprived cancer cells to supplementation with the non-human Neu5Gc form of sialic acid with levels of sialoglyconjugate display reaching levels of 6-fold higher compared to normal cell lines. The enhanced incorporation of Neu5Gc into nutrient-deprived cancer cells compared to their non-cancerous counterparts helps explain the selective display of this dietary sugar in tumors [45].

Looking forward, the enhanced “therapeutic window” afforded by nutrient-deprivation holds potential to be applied to other non-human sialic acids including non-natural variants such as azido-sialic acids [46] increasingly used in metabolic glycoengineering applications [16]. Already selective display of azido sialic acids have been reported in tumors in animal models [17] and our current report provides mechanistic insight into these studies insofar as nutrient deprivation commonly found in tumor environments combined with exogenous provision of nutritional supplements to augment sialylation explains the overexpression on non-natural sialic acids in cancerous tissues

5. Conclusion

Developing tumors often face nutrient deprivation, which can lead to rapid loss of various types of glycans that promote cancer progression. This report describes how exogenously-supplied sialic acid can not only restore cell surface sialylation but also supports a

Author Manuscript Author Manuscript Author Manuscript Author Manuscript

multifaceted response wherein this sugar increases UDP-GlcNAc levels and the transcription of a suite of enzymes (sialyltransferases) and cancer-associated proteins (MUC1 and EGFR) that enhance cell migration endpoints important in metastasis. This work also illustrates how a cancer cell's ability to utilize extracellular and "non-human" sialic acids opens the door to new diagnostic and therapeutic approaches. Overall, the work provides insights into how sialic acid utilization complements the Warburg effect whereby cancer cells are ubiquitously characterized by abnormally high glucose metabolism.

Supplementary Material

Refer to Web version on PubMed Central for supplementary material.

Acknowledgments

This study was supported by the Ministry of Science and Education of the Republic of Kazakhstan grant (0068GF) to L.B.D., grants from the National Institute of Health (NIH) (R15ES021079-01) and the National Science Foundation (1334417) to C.Z.L.; a NIH grant (R01CA112314) to K.J.Y. and a NIH grant (R41CA141970-01A2) to H.A.

References

1. Warburg O, Posener K, Negelein E. Ueber den Stoffwechsel der Tumoren. Biochemische Zeitschrift. 1924; 152:319–344.
2. Hanahan D, Weinberg RA. Hallmarks of cancer: the next generation. Cell. 2011; 144(5):646–674. [PubMed: 21376230]
3. Vaupel P, Kallinowski F, Okunieff P. Blood flow, oxygen and nutrient supply, and metabolic microenvironment of human tumors: a review. Cancer Res. 1989; 49(23):6449–6465. [PubMed: 2684393]
4. Yin J, et al. Hypoxic culture induces expression of sialin, a sialic acid transporter, and cancer-associated gangliosides containing non-human sialic acid on human cancer cells. Cancer Res. 2006; 66(6):2937–2945. [PubMed: 16540641]
5. Lau KS, Dennis JW. *N*-Glycans in cancer progression. Glycobiology. 2008; 18(10):750–760. [PubMed: 18701722]
6. Slawson C, Hart GW. O-GlcNAc signalling: implications for cancer cell biology. Nat Rev Cancer. 2011; 11:678–684. [PubMed: 21850036]
7. Lajoie P, Goetz JG, Dennis JW, Nabi IR. Lattices, rafts, and scaffolds: domain regulation of receptor signaling at the plasma membrane. J Cell Biol. 2009; 185(3):381–385. [PubMed: 19398762]
8. Oetke C, et al. Evidence for efficient uptake and incorporation of sialic acid by eukaryotic cells. Eur J Biochem. 2001; 268(16):4553–4561. [PubMed: 11502217]
9. Tangvoranuntakul P, et al. Human uptake and incorporation of an immunogenic nonhuman dietary sialic acid. Proc Natl Acad Sci U S A. 2003; 100(21):12045–12050. [PubMed: 14523234]
10. Angata T, Varki A. Chemical diversity in the sialic acids and related a-keto acids: an evolutionary perspective. Chem Rev. 2002; 102(2):439–469. [PubMed: 11841250]
11. Irie A, Koyama S, Kozutsumi Y, Kawasaki T, Suzuki A. The molecular basis for the absence of *N*-glycolylneuraminic acid in humans. J Biol Chem. 1998; 273(25):15866–15871. [PubMed: 9624188]
12. Varki A. Sialic acids as ligands in recognition phenomena. FASEB J. 1997; 11:248–255. [PubMed: 9068613]
13. Schultz MJI, Swindall AF, Bellis SL. Regulation of the metastatic cell phenotype by sialylated glycans. Cancer Metastasis Rev. 2012; 31:501–518. [PubMed: 22699311]

Author Manuscript Author Manuscript Author Manuscript Author Manuscript

14. Almagro-Moreno S, Boyd EF. Sialic acid catabolism confers a competitive advantage to pathogenic *Vibrio cholerae* in the mouse intestine. Infect Immun. 2009; 77(9):3807–3816. [PubMed: 19564383]
15. Wang B, Brand-Miller J. The role and potential of sialic acid in human nutrition. European J Clin Nutr. 2003; 57:1351–1369. [PubMed: 14576748]
16. Du J, et al. Metabolic glycoengineering: sialic acid and beyond. Glycobiology. 2009; 19(12):1382–1401. [PubMed: 19675091]
17. Neves AA, et al. Imaging sialylated tumor cell glycans *in vivo*. FASEB J. 2011; 25(8):2528–2537. [PubMed: 21493886]
18. Badr HA, et al. Preferential lectin binding of cancer cells upon sialic acid treatment under nutrient deprivation. Appl Biochem Biotechnol. 2013; 171(4):963–974. [PubMed: 23912210]
19. Geisler C, Jarvis DL. Effective glycoanalysis with Maackia amurensis lectins requires a clear understanding of their binding specificities. Glycobiology. 2011; 21(8):988–993. [PubMed: 21863598]
20. Bonay P, Munro S, Fresco M, Alacorn B. Intra-Golgi transport inhibition by Megalomicin. J Biol Chem. 1996; 271:3719–3726. [PubMed: 8631986]
21. Bardor M, Nguyen DH, Diaz S, Varki A. Mechanism of uptake and incorporation of the non-human sialic acid *N*-glycolylneuraminic acid into human cells. J Biol Chem. 2005; 280(6):4228–4237. [PubMed: 15557321]
22. Nakajima K, et al. Simultaneous determination of nucleotide sugars with ion-pair reversed-phase HPLC. Glycobiology. 2010; 20(7):865–871. [PubMed: 20371511]
23. Ghaderi D, Taylor RE, Padler-Karavani V, Diaz S, Varki A. Implications of the presence of N-glycolylneuraminic acid in recombinant therapeutic glycoproteins. Nat Biotechnol. 2010; 28(8):863–867. [PubMed: 20657583]
24. Qian J, et al. α2,6-Hyposialylation of c-Met abolishes cell motility of ST6Gal-I-knockdown HCT116 cells. Acta Pharmacol Sin. 2009; 30(7):1039–1045. [PubMed: 19483716]
25. Münster AK, et al. Mammalian cytidine 5′-monophosphate N-acetylneuraminic acid synthetase: a nuclear protein with evolutionarily conserved structural motifs. Proc Natl Acad Sci U S A. 1998; 95(16):9140–9145. [PubMed: 9689047]
26. Recchi MA, Harduin-Lepers A, Boilly-Marer Y, Verbert A, Delannoy P. Multiplex RT-PCR method for the analysis of the expression of human sialyltransferases: application to breast cancer cells. Glycoconj J. 1998; 15(1):19–27. [PubMed: 9530953]
27. Jin C, et al. Cooperative interaction between the MUC1-C oncoprotein and the Rab31 GTPase in estrogen receptor-positive breast cancer cells. PLoS One. 2012; 7(7):e39432. [PubMed: 22792175]
28. Hsia TC, et al. Lapatinib-mediated cyclooxygenase-2 expression via epidermal growth factor receptor/HuR interaction enhances the aggressiveness of triple-negative breast cancer cells. Mol Pharmacol. 2013; 83(4):857–869. [PubMed: 23355539]
29. Guha P, et al. Nicotine promotes apoptosis resistance of breast cancer cells and enrichment of side population cells with cancer stem cell-like properties via a signaling cascade involving galectin-3, α9 nicotinic acetylcholine receptor and STAT3. Breast Cancer Res Treat. 2014; 145(1):5–22. [PubMed: 24668500]
30. Almaraz RT, et al. Metabolic flux increases glycoprotein sialylation: implications for cell adhesion and cancer metastasis. Mol Cell Proteomics. 201210.1074/mcp.M1112.017558
31. Yang NC, et al. A convenient one-step extraction of cellular ATP using boiling water for the luciferin-luciferase assay of ATP. Anal Biochem. 2002; 306:323–327. [PubMed: 12123672]
32. Mathew MP, et al. Metabolic glycoengineering sensitizes drug-resistant pancreatic cancer cells to tyrosine kinase inhibitors erlotinib and gefitinib. Bioorg Med Chem Lett. 2015; 25(6):1223–1227. [PubMed: 25690786]
33. Luchansky SJ, Yarema KJ, Takahashi S, Bertozzi CR. GlcNAc 2-epimerase can serve a catabolic role in sialic acid metabolism. J Biol Chem. 2003; 278(10):8036–8042.
34. Badr HA, et al. Lectin approaches for glycoproteomics in FDA-approved cancer biomarkers. Expert Rev Proteomics. 2014; 11(2):227–236. [PubMed: 24611567]

Author Manuscript Author Manuscript Author Manuscript Author Manuscript

35. Guha P, et al. Cod glycopeptide with picomolar affinity to galectin-3 suppresses T-cell apoptosis and prostate cancer metastasis. Proc Natl Acad Sci U S A. 2013; 110(13):5052–5057. [PubMed: 23479624]
36. Liu C, et al. Live cell integrated surface plasmon resonance biosensing approach to mimic the regulation of angiogenic switch upon anti-cancer drug exposure. Anal Chem. 2014; 86(15):7305–7310. [PubMed: 25005895]
37. Nauman DA, Bertozzi CR. Kinetic parameters for small-molecule drug delivery by covalent cell surface targeting. Biochim Biophys Acta. 2001; 1568:147–154. [PubMed: 11750762]
38. Zachara NE, Butkinaree C, Hart GW. O-GlcNAc: A new paradigm for modulating cellular responses to stress. Glycobiology. 2003; 13(11):833.
39. Lewis BA, Hanover JA. O-GlcNAc and the epigenetic regulation of gene expression. J Biol Chem. 2014; 289:34440–34448. [PubMed: 25336654]
40. Wang PH, Lee WL, Juang CM, Yang YH, Lo WH, Lai CR, Hsieh SL, Yuan CC. Altered mRNA expressions of sialyltransferases in ovarian cancers. Gynecol Oncol. 2005; 99:631–639. [PubMed: 16112178]
41. Bos PD, Zhang XH, Nadal C, Shu W, Gomis RR, Nguyen DX, Minn AJ, van de Vijver MJ, Gerald WL, Foekens JA, Massagué J. Genes that mediate breast cancer metastasis to the brain. Nature. 2009; 459:1005–1009. [PubMed: 19421193]
42. Malagolini N, Trinchera M, Chiricolo M. Sialosignaling: sialyltransferases as engines of self-fueling loops in cancer progression. Biochim Biophys Acta. 2014; 1840:2752–2764. [PubMed: 24949982]
43. Fuster MM, Esko JD. The sweet and sour of cancer: glycans as novel therapeutic targets. Nat Rev Cancer. 2005; 5(7):526–542. [PubMed: 16069816]
44. Picco G, et al. Over-expression of ST3Gal-I promotes mammary tumorigenesis. Glycobiology. 2010; 20(10):1241–1250. [PubMed: 20534593]
45. Gabri MR, Otero LL, Gomez DE, Alonso DF. Exogenous incorporation of neugc-rich mucin augments n-glycolyl sialic acid content and promotes malignant phenotype in mouse tumor cell lines. J Exp Clin Cancer Res. 2009; 28:146. [PubMed: 19951433]
46. Saxon E, Bertozzi CR. Cell surface engineering by a modified Staudinger reaction. Science. 2000; 287(5460):2007–2010. [PubMed: 10720325]

Author Manuscript Author Manuscript Author Manuscript Author Manuscript

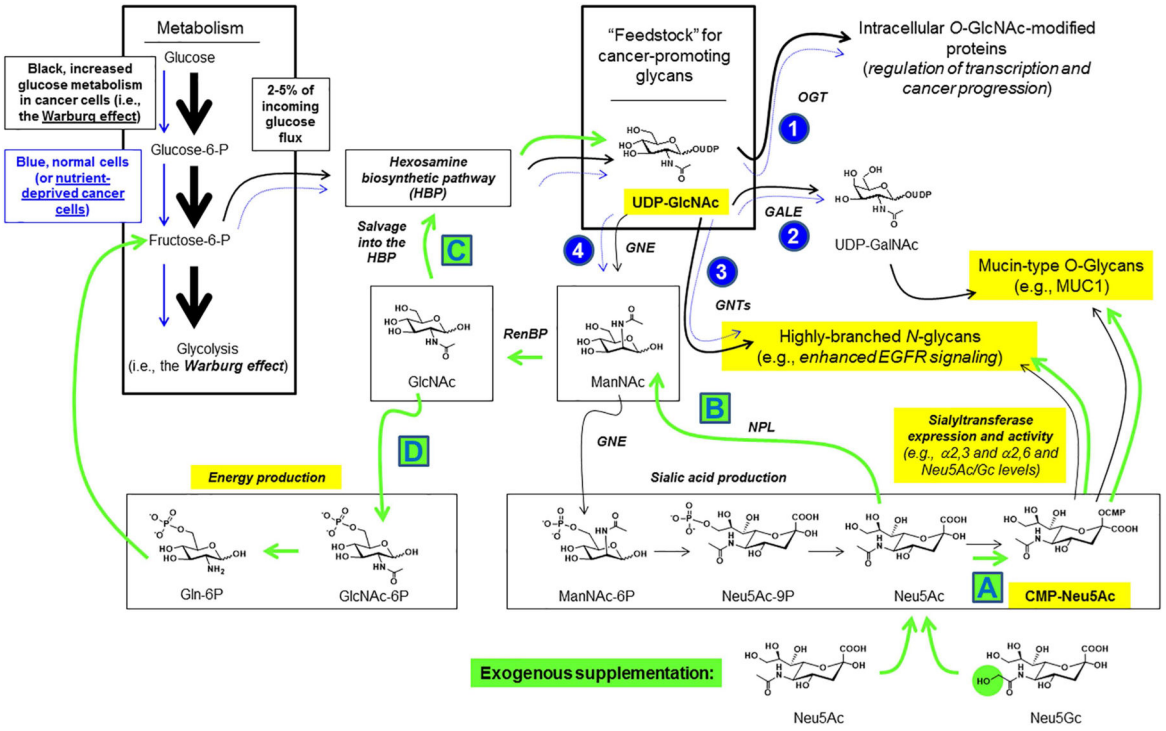

Figure 1. Monosaccharide metabolism and supplementation strategies

Cancer cells are characterized by the "Warburg effect" wherein the cells use greatly increased levels of glucose (indicated by the black arrows throughout the diagram). One consequence of increased glucose utilization by cancer cells is increased production of UDP-GlcNAc, which promotes cancer progression by several complementary glycan-based mechanisms including (**1**) O-GlcNAc protein modification, (**2**) production of mucin-type O-glycans such as those that decorate MUC1, (**3**) activation of GlcNAc transferases 4 and 5, which produce highly-branched N-glycans linked to cancer including through promotion of EGFR signaling, and (**4**) sialic acid biosynthesis via ManNAc production. In all of these cases, lower glucose uptake found naturally in normal cells or induced by nutrient deprivation in cancer cells is expected to reduce UDP-GlcNAc levels and attenuate these cancer-promoting mechanisms (as indicated schematically by the smaller blue arrows). Supplementation of nutrient-deprived cells with sialic acids (e.g., either Neu5Ac or Neu5Gc, bottom) leads to several plausible outcomes that can counteract the effects of nutrient deprivation and maintain the production of cancer-promoting glycans (indicated with the green arrows) including (**A**) direct incorporation into cellular glycans, (**B**) catabolism to ManNAc, which can be re-used for sialic acid production (not shown) or conversion to GlcNAc. In turn, GlcNAc can (**C**) be salvaged by the HBP and used to replenish cellular supplies of UDP-GlcNAc or (**D**) be routed into a pathway that creates fructose-6-phosphate that can be used for energy production. Specific endpoints investigated in this report are highlighted in yellow.

Author Manuscript Author Manuscript Author Manuscript Author Manuscript

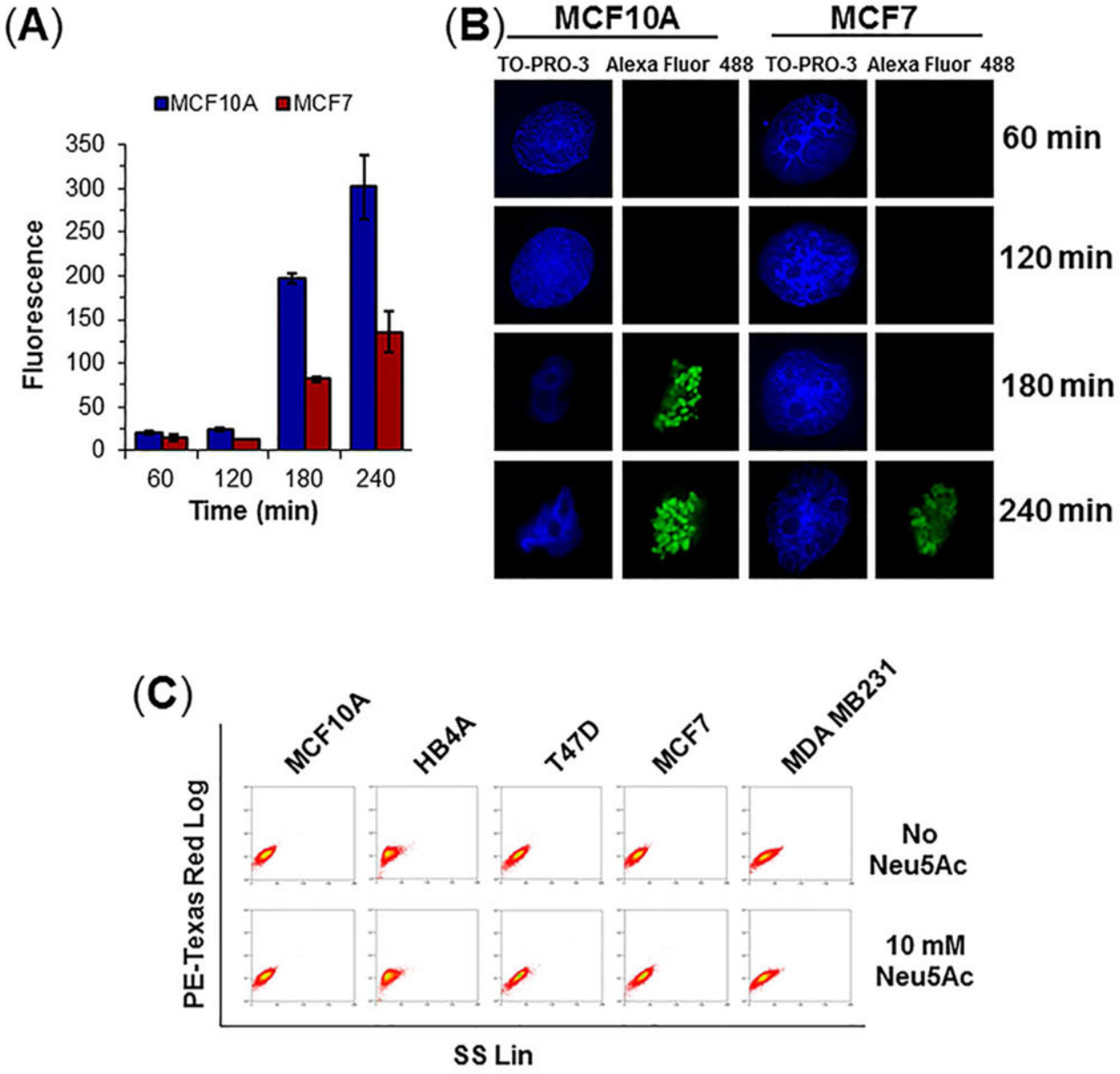

Figure 2. Optimization of nutrient depletion conditions

(**A**) TUNEL assay for apoptosis. Cells were treated with 10 mM Neu5Ac for varying time points followed by treatment with BrdUTP and immuno-stained with anti-BrdU antibody-Alexa Fluor 488 conjugate and analyzed by flow cytometry. The level of fluorescence indicates the degree of DNA damage. (**B**) Cell imaging. Anti-BrdU Ab-Alexa Fluor 488 labeled cells were visualized under confocal microscope. Magnification: 100×. (**C**) Cytograms showing determination of live cells. Cells were treated with or without 10 mM Neu5Ac in nutrient deprived condition for 2 h and stained with 1 mg/mL propidium iodide (PI) on ice for 20 min and analyzed by flow cytometry in PE-Texas Red setting.

Author Manuscript Author Manuscript Author Manuscript Author Manuscript

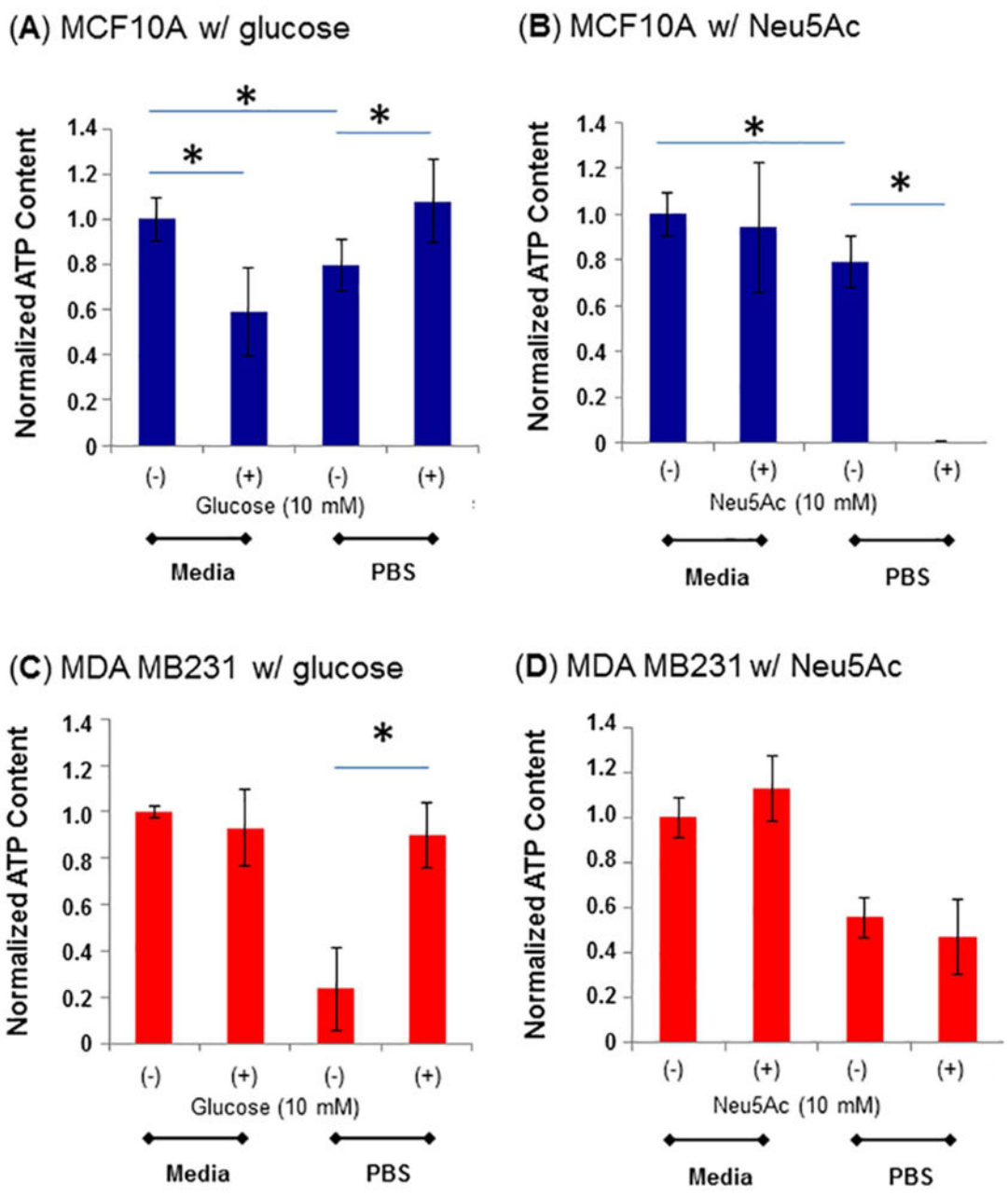

Figure 3. Measurement of ATP levels in MCF10A

(**A**, **B**) and MDA MB231 (**C**, **D**) cells in normal media or after nutrient-deprivation, with either glucose (**A**, **C**) or Neu5Ac (**B**, **D**) supplementation. The data are representative of three independent experiments with S.D. indicated by error bars and *p* values were determined by two-tailed student t-test and <0.05 is indicated by one asterisk (significant between the two as shown by each horizontal bar).

Author Manuscript Author Manuscript Author Manuscript Author Manuscript

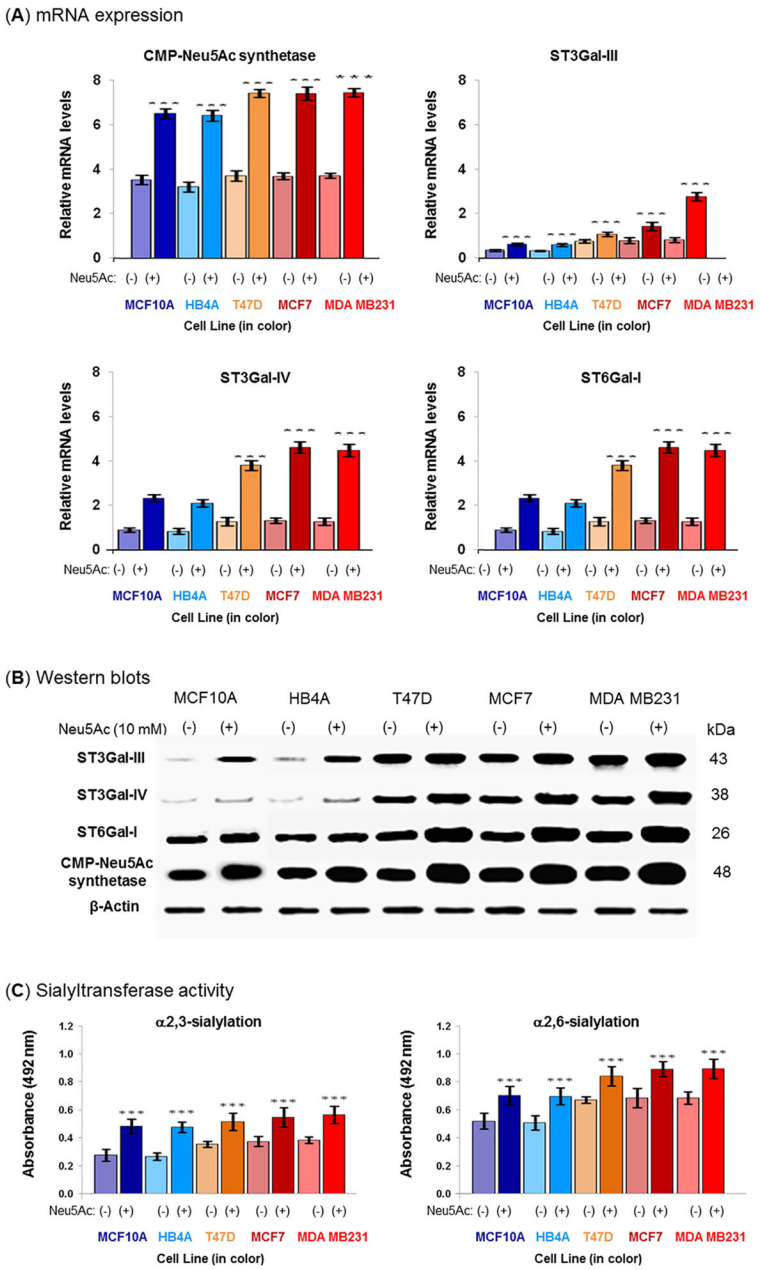

Figure 4. Quantitative RT-PCR, western blot detection of ST3Gal-III, ST3Gal-IV, ST6Gal-I, and CMP-Neu5Ac synthetase, and sialyltransferase activity

Cells were nutrient-deprived in the presence or absence of 10 mM Neu5Ac for 2 h and the (**A**) relative mRNA expression of CMP-Neu5Ac synthetase, ST3Gal-III, ST3Gal-IV, and ST6Gal-I was assessed by quantitative RT-PCR and (**B**) the protein expression of these genes was analyzed by Western blot. The results were normalized to *β*-actin expression. The data are representative of five independent experiments with S.D. indicated by error bars. *P* values are determined by two-tailed student t-test and <0.05, <0.01 and <0.001 are indicated by one, two and three asterisks, respectively compared to the corresponding untreated cells. For negative control Western blot experiments, PBS was used instead of primary antibodies.

Author Manuscript Author Manuscript Author Manuscript Author Manuscript

Each antibody resulted a single band corresponding to the antigen molecular weight, shown on the right. Negative controls did not result in any bands. (**C**) Detection of sialyltransferase activity. Cells were lysed and the same amounts of proteins were used on solid phase assays using asialofetuin precoated plates. The α2→3- and α2→6-sialylated glycans of resultant fetuin was detected with biotinylated MAL-I and biotinylated SNA, respectively. The data are representative of five independent experiments with S.D. indicated by error bars. *p* values are determined by two-tailed student t-test and <0.05, <0.01 and <0.001 are indicated by one, two and three asterisks, respectively.

Author Manuscript Author Manuscript Author Manuscript Author Manuscript

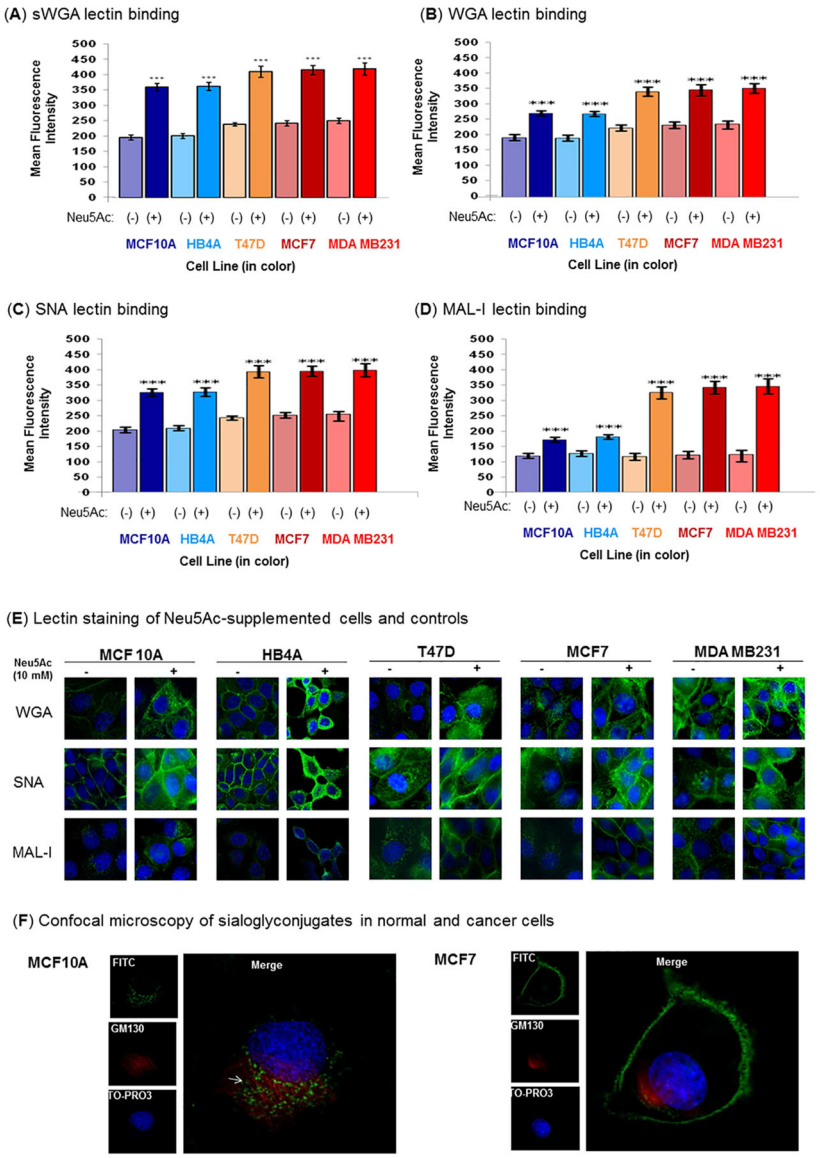

Figure 5. Flow cytometric analysis of lectin binding

Cells were treated in the presence or absence of 10 mM Neu5Ac under nutrient deprivation for 2 h. The α2→3 and α2→6 sialylated glycans were stained with the fluorescein isothiocyanate-labeled lectins, sWGA (**A**), WGA (**B**), SNA (**C**), and MAL-I (**D**) followed by analysis on a flow cytometer. (**E**). Lectin staining followed by cell imaging. Cells were treated for 2 h in the presence or absence of Neu5Ac (10 mM) under nutrient deprivation and stained for 1 h with FITC-labeled lectins (WGA, SNA, and MAL-I) at concentration of 5 μg/mL (green fluorescence). Cells were further treated with 50 μg/ml ribonuclease A and the nuclei were counter-stained with TO-PRO-3 (blue fluorescence), Images are shown at 60x magnification. (**F**) Confocal imaging of MAL-I staining. Co-staining of Neu5Ac treated (as above) MCF10A and MCF7 with MAL-I-FITC (green) and anti-GM130 antibody (golgi marker) (red). The white arrow represents merge color. 100x magnification.

Author Manuscript Author Manuscript Author Manuscript Author Manuscript

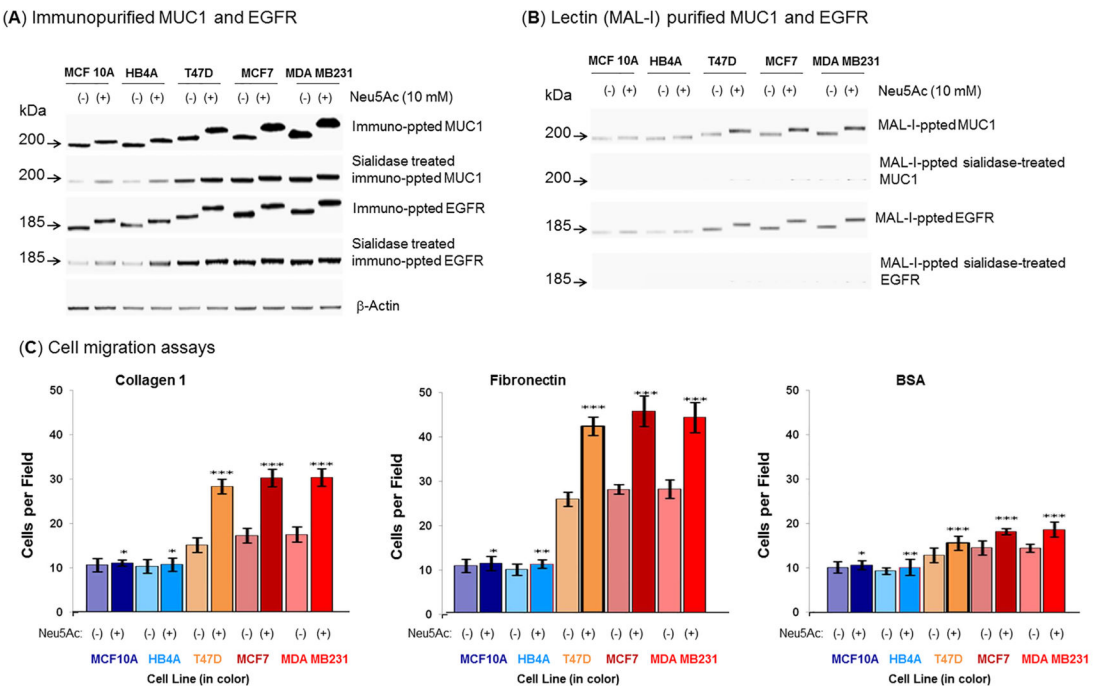

Figure 6. Examination of sialylation of MUC1 and EGFR on normal and malignant cells after sialic acid treatment under nutrient deprivation and cell migration

(**A**) Equal amount (100 μg) of each cell extract was subjected to immuno-precipitation with anti-MUC1 and anti-EGFR antibodies and the precipitated proteins were subjected to Western blot and immuno-detection with the respective antibody. In parallel, equal amount of each crude protein extract was desialylated and similar precipitation was carried out. (**B**) Equal amount of immuno-precipitated proteins (MUC1 and EGFR) as described above was subjected to MAL-I precipitation and detected on W. blot as described above. (C) Cell migration. Migration assays were performed on confluent monolayers treated or not treated with 10 mM Neu5Ac under nutrient deprived condition. Data are shown as the number of cells that migrated into a 300×300 micron area along the center of the wound in 24 hours. The data are representative of five independent experiments with S.D. indicated by error bars. *P* values are determined by two-tailed student t-test and <0.05, <0.01 and <0.001 are indicated by one, two and three asterisks, respectively compared to the corresponding untreated cells.

Author Manuscript

Author Manuscript

Author Manuscript

Author Manuscript

Table 1

Quantitation of nucleotide sugars, surface Neu5Ac, and Neu5Gc

Cell line	A CMP-Neu5Ac	B Neu5Ac	C UDP-GlcNAc	D Neu5Gc
A) Untreated				
MCF10A	0.29 ± 1.05	1.29 ± 1.60	2.69 ± 2.1	0.136 ± 0.42
HB4A	0.33 ± 0.95	1.33 ± 1.43	2.80 ± 3.6	0.151 ± 0.652
T47D	0.422 ± 1.18	2.53 ± 1.61	3.10 ± 2.3	0.19 ± 0.811
MCF7	0.75 ± 1.32	2.82 ± 1.54	4.95 ± 6.6	0.254 ± 0.64
MDA MB231	0.78 ± 1.58	2.85 ± 2.70	5.01 ± 5.2	0.298 ± 0.897
B) Treated				
MCF10A	0.45 ± 1.92	1.81 ± 2.15	5.18 ± 2.52	0.177 ± 0.31
HB4A	0.51 ± 1.33	1.83 ± 2.09	5.32 ± 7.41	0.182 ± 0.73
T47D	1.06 ± 1.42	5.07 ± 4.56	6.513 ± 5.3	0.608 ± 0.675
MCF7	2.253 ± 1.77	7.05 ± 3.95	12.40 ± 3.66	1.58 ± 0.912
MDA MB231	2.496 ± 2.63	7.12 ± 4.91	12.53 ± 4.2	1.79 ± 0.982

Cells were treated in the presence or absence of 10 mM Neu5Ac for 2 h under nutrient deprivation and quantity of CMP-Neu5Ac (A), surface Neu5Ac (B), and UDP-GlcNAc (C) was determined as described in Methods. For quantitation of surface Neu5Gc, cells were treated with 10 mM Neu5Gc for 2 h under nutrient deprivation. The content of CMP-Neu5Ac, Neu5Ac, UDP-GlcNAc and Neu5Gc was shown in nano mole per mg cell protein from five independent experiments.